

Surfactant CTAB Controlled Synthesis of ZIF-8 Supported Pt for Oxygen Reduction Catalyst

Yufeng Ren¹, Weiling Luan^{1*}, Tao Jiang¹

¹ Key Laboratory of Pressure Systems and Safety (MOE), School of Mechanical and Power Engineering, East China University of Science and Technology, Shanghai 200237, China.

ABSTRACT

Oxygen reduction reaction (ORR) is an important electrochemical reaction in fuel cells (FCs). Until now, Pt and its alloys are still the best materials for ORR. However, the problem lies on how to prepare a high-performance catalyst with the lowest usage of Pt. Metal organic frameworks (MOFs) that represented by Zeolitic imidazolate framework (ZIFs) have been used as precursors for efficient transition metal-nitrogen-carbon (M-N-C, M=Fe, Co, Mn, et. al) catalysts ORR catalysts. However, these catalysts are generally reported to suffer from poor activity. In this paper, a low Pt catalyst Pt-NC-900 was synthesized by dispersing Pt on cubic ZIF-8 with highly usage for Pt. Cetyltrimethylammonium bromide (CTAB) was used to control synthesize cubic ZIF-8 in the aqueous phase. This synthesis method was a green process because no methanol was required. As synthesized ZIF-8 displayed a large specific surface area of 1870 m²/g. Subsequently, Pt was loaded on the carbon support with high pyridinic N content that obtained through heat treatment atmosphere and temperature optimization. The sample was treated under N₂ atmosphere at 900°C to obtain Pt-NC-900. It showed an optimal electrochemical performance with a half-wave potential ($E_{1/2}$) of 0.84 V, which is 10 mV higher than Pt/C20% catalyst. and the Pt-NC-900 also showed a higher mass activity (0.207 A/mg_{Pt}) than Pt/C20%. The excellent ORR performance could be attributed to the Pt active centers, large specific surface area, rich pore structure, and high pyridinic-N content.

Keywords: low Pt; oxygen reduction reaction; metal organic framework; catalyst

1. INTRODUCTION

Fuel cells use hydrogen as fuel have the advantages of high efficiency, low pollution and noise, and reliable operation [1]. Like lithium battery vehicles, they are considered as a possible alternative to traditional vehicles and have received extensive attention from various countries. Oxygen reduction reaction (ORR) is an important electrochemical reaction in fuel cells, which has high requirements on catalysts. Traditional platinum-based catalysts have excellent performance in catalytic activity and stability. However, high cost is the most important reason that hinders the commercialization of proton exchange membrane fuel cells [2]. Therefore, the reduce of Pt for Pt-based catalysts with high-performance is the key to enhance the hydrogen energy applications [3].

In recent years, researchers have focused on non-platinum catalysts. Among them, metal-organic frameworks (MOFs) are generally used as potential precursors for the preparation of transition metal catalysts because of their large specific surface area and rich pore structure [4]. These catalysts provided more attachment points for active components and excellent material transport capabilities. Especially ZIF-8, which is a Sodalite (SOD) topological structure formed by zinc ion and 2-methylimidazole linker. The NC catalyst prepared by direct pyrolysis of ZIF-8 has been proved to have a unique catalytic ability for ORR in alkaline medium [5]. In addition, the Zn metal sites in ZIF-8 can be easily replaced by other transition metals (such as Fe, Ni, Co) by solvent method, and further pyrolyzed to form M-N-C catalysts [6]. But these non-Pt catalysts face the problems of low catalytic activity and poor stability, therefore cannot completely replace Pt catalyst. Therefore, low Pt catalyst is a feasible method to solve the practical application of fuel cell [7-9]. In this article,

we modified the experiment referred to latest research using ZIF-8 as a precursor to synthesize catalysts[10]. Our cubic ZIF-8 (synthesis controlled by CTAB) is synthesized by aqueous phase, abandoning the traditional methanol solvent synthesis method, which is environmentally green. The effect of surfactants on the morphology of ZIF-8 was explored. Then during the carbonization process, the heat treatment atmosphere and temperature were optimized, and the changes in the pores, specific surface area and N species of the carbon support under different heat treatment conditions were investigated. Pt was doped into the carbon materials that resulted from the heat treatment of cubic ZIF-8 using solvent impregnation method. The Pt-NC catalyst that was obtained after the second calcination inherited the cubic structure. It performed a high ORR activity with $E_{1/2} = 0.84$ V, and good stability with only 70 mV decline after 5000 cycles. Moreover, it has the optimal Pt usage with the mass percentage of 12%.

2. EXPERIMENTAL SECTION

2.1 Material and methods

Zinc nitrate hexahydrate, 2-methylimidazole, cetyltrimethylammonium bromide (CTAB), Myristyltrimethylammonium bromide (TTAB), chloroplatinic acid hexahydrate, sodium borohydride, ethylene glycol, ethanol and perchloric acid (70 – 72%) were purchased from Aladdin and used without further purification.

2.2 Synthesis of ZIF-8

To synthesize ZIF-8, 4.8 g of dimethylimidazole was dissolved in 60 mL of ultrapure water. Then, 350 mg of zinc nitrate hexahydrate ($Zn(NO_3)_2 \cdot 6H_2O$) and a certain amount of CTAB/TTAB were dissolved in 20 mL of ultrapure water, stirred for 20 minutes until uniform and transparent, and quickly added to the previous solution. After stirring at room temperature for 10 minutes, the milky white solution was transferred to a 100 mL polytetrafluoroethylene-lined stainless steel reactor, kept at $120^\circ C$ for 6 hours, and then naturally cooled to room temperature. The solution was centrifuged at 8000rpm, washed twice with ultrapure water, and the final solid product was dried in a vacuum oven at $60^\circ C$ for 12h.

2.3 Heat treatment of ZIF-8

Put ZIF-8 into the ceramic boat and send it into the tube furnace. The heat treatment temperature was set to $T^\circ C$ ($T=700,800,900,1000$), the heating rate was $5^\circ C/min$ under N_2 or Ar atmosphere, and the finished black powder is named NC-T.

2.4 Pt load process

First, 100 mg of NC-T was mixed with 20 ml of ethylene glycol under stirring for 30 min. Then, 600 ml of H_2PtCl_6/H_2O (0.193 M) were added to the above solution, then vigorously stirred for 120 min. Finally, 10 ml of aqueous solution of 0.6 M $NaBH_4$ was slowly added dropwise to the above solution, and the resulting solution was stirred rapidly for 30 min. The product was separated at 6000rpm and washed twice with ethanol. And the final solid product was dried again in a vacuum oven at $60^\circ C$ overnight.

2.5. Materials characterization

XRD patterns of all samples were obtained using on Rigaku 2550VB. The morphology of all samples was observed using field emission scanning electron microscopy (FESEM, Hitachi Limited S-4800). For chemical and compositional analysis, X-ray photoelectron spectroscopy (XPS, Thermo ESCALAB250) and inductively coupled plasma atomic emission spectroscopy (ICP-AES, Baird PS-6) were used. The degree of graphitization of the electrocatalysts was investigated by Raman spectroscopy (LabRAM ARAMIS). The specific surface areas of different samples were measured by using the Brunauer – Emmett – Teller method (BET, AS-1C-VP).

2.6. Electrochemical measurements

In order to study the electrochemical activity and stability of the catalyst, a three-electrode system was used on the CHI 760E electrochemical workstation (CH Instruments, Chenhua, China) to perform cyclic voltammetry (CV) and linear voltammetry (LSV) tests on the catalyst. During the test, graphite electrode and Ag/AgCl electrode are used as counter electrode and reference electrode, respectively, and rotating disk electrode is used as working electrode. Typical catalyst ink preparation process: Add 490ml of isopropanol, 490ml of ultrapure water and 20ml of 5 wt% Nafion solution to 3mg of catalyst powder, and sonicate the mixed solution for 1h. Drop 3mg of uniform ink on the rotating disk electrode (previously sanded and cleaned with $0.3 \mu m$ Al_2O_3 powder). Select 0.1M $HClO_4$ as the test solution, and filled with O_2 30min to make it saturated. The electrode was activated with 40 cycles of

cyclic voltammetry (CV) at a scanning rate of 0.1 V s^{-1} between -0.2 V and 1 V at room temperature. The CV curves were measured at a scanning rate of $0.05 \text{ V} \cdot \text{s}^{-1}$. In the same potential range, use a sweep rate of $0.01 \text{ V} \cdot \text{s}^{-1}$ to perform linear sweep voltammetry (LSV) measurement. All potentials have been switched to reversible hydrogen electrode (RHE)

2. EXPERIMENT RESULTS AND DISCUSSION

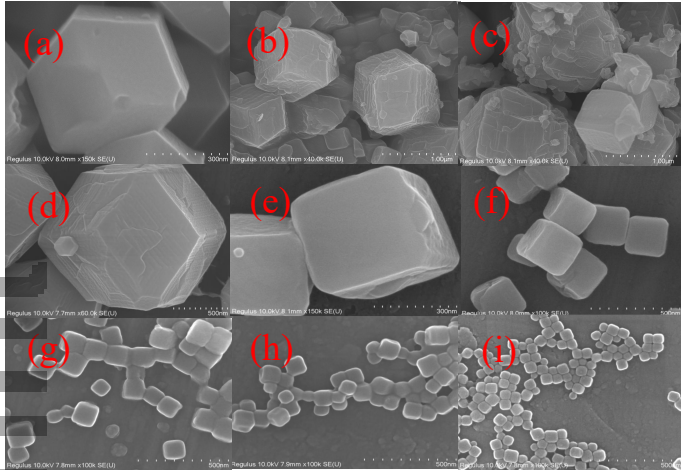


Fig.1. The SEM image of the synthesized ZIF-8 crystal (a) using methanol as the solvent (b) using water as the solvent and adding (c) TTAB and different amounts of CTAB (d) no addition, (e) 3mg, (f) 6mg, (g) 9mg, (h) 12mg, (i) 15mg.

A ZIF-8 precursor was prepared in the aqueous phase and compared with the traditional methanol solvent preparation method (Fig.1a-b). The ZIF-8 synthesized with methanol as a solvent has a rhombic dodecahedron structure with a size of about 400nm, uniform and regular appearance, while the ZIF-8 synthesized with water as a solvent has uneven size, rough surface. The particle size generally larger than $1 \mu\text{m}$. After the addition of surfactant, the morphology changed significantly. The particles showed a cubic structure. But the size of the sample with TTAB was still uneven (Fig.1c), while the morphology of the sample with CTAB was more uniform and regular (Fig.1e). In order to explore the effect of different particle sizes on the catalyst, we controlled the amount of CTAB introduced (Fig.1d-i), and the particle size was reduced from $1 \mu\text{m}$ to 40 nm. When the amount of CTAB added is 6mg, the particle size is adjusted to be about 300nm, which is close to ZIF-8 synthesized with methanol as a solvent. The subsequent electrochemical characterization also verified that the 300nm carrier is optimal. The XRD pattern shows that there is no significant difference between the cubic ZIF-8 and the dodecahedral ZIF-8 made from methanol (Fig.2).

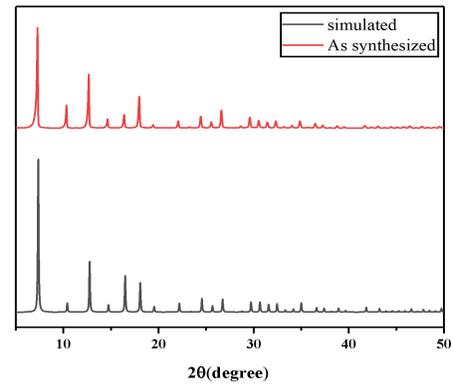


Fig 2 XRD patterns of 6mg control synthesis cube ZIF-8

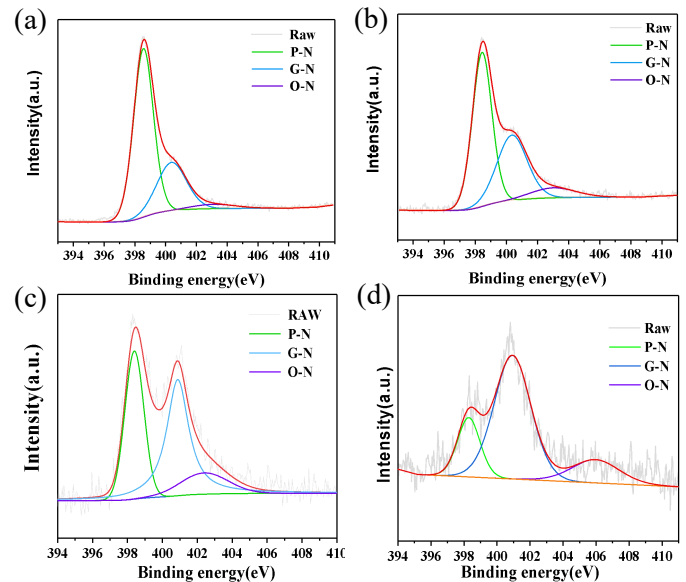


Fig3 XPS of N 1s spectra of (a)NC-700; (b)NC-800; (c)NC-900; (d)NC-1000

The conductivity of the prepared ZIF-8 is poor, so it needs to be further carbonized to increase its graphitization degree. We put this precursor at different temperatures (700°C , 800°C , 900°C , 1000°C) and different atmospheres (N_2 and Ar) carbonization, in which the samples treated in N_2 atmosphere at 900°C showed the best performance in the subsequent electrochemical test. Taking into account the influence of the type of N in the catalyst on the catalytic activity, we proceeded to X-ray photoelectron spectroscopy deconvoluted the N element of NC-T. The XPS test shows that three typical states of N (pyridine-N $398.4 \pm 0.1 \text{ eV}$, graphitized-N $400.9 \pm 0.1 \text{ eV}$ and N-oxide group $402.4 \pm 0.3 \text{ eV}$) can be seen from the Fig.3. NC-700 has the highest content of pyridine-N, followed by graphite-N, and the lowest content of nitrogen oxides. As the temperature increases, the content of pyridine-N decreases and the content of graphite-N increases. Pyridine-N is considered to have certain catalytic

activity and can also be used to support Pt nanoparticles, and the increase in graphitization also contributes to the enhancement of electrical conductivity. An excellent catalyst carrier should take both aspects into consideration. NC-900 has higher pyridine N and graphite N, so it has better platinum loading capacity and conductivity.

The Raman spectra (Fig. 4) of NC-700, NC-800, NC-900, NC-1000 revealed two characteristic peaks of D (1340 cm^{-1}) and G (1590 cm^{-1}) bands of carbon with intensity ratios I_D/I_G of 1.07, 1.04, 1.02, and 1.01, respectively. This shows that when the temperature increases, as the degree of graphitization of the material increases, the composition of the disordered carbon also increases, which can be used to provide more Pt loading sites, thereby improving the ORR performance of the catalyst.

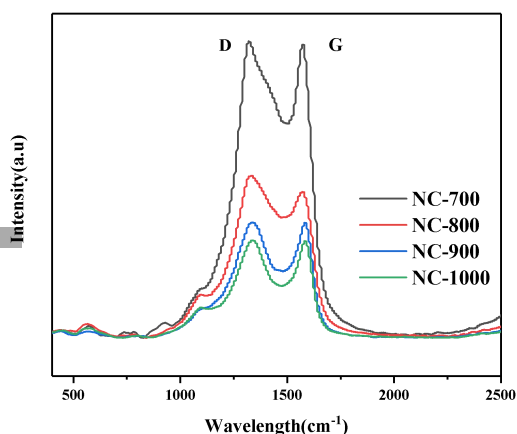


Fig. 4 Raman spectrum of NC-700, NC-800, NC-900, NC-1000

Specific surface area and pore size distribution were assessed via the measurements of nitrogen adsorption-desorption isotherms. The curves showed obvious type I curves, which proved that the samples were mainly micropores. The specific surface area was assessed via the measurements of nitrogen adsorption-desorption isotherms (Tab.1). It can be seen that the change trend of its specific surface area is consistent with the heat treatment temperature. The largest Pt loading capacity is NC-1000 (14.1%). Although it has a higher Pt content, in the following electrochemical characterization, the sample treated at $1000\text{ }^\circ\text{C}$ is not the best performance. This may be due to the massive collapse of the pores of ZIF-8 after exceeding the boiling point of Zn ($908\text{ }^\circ\text{C}$), causing some active sites to be blocked.

Tab.1. Specific surface area and Pt loading capacity of samples processed at different temperatures

Heat treatment temperature/ $^\circ\text{C}$	700	800	900	1000
Specific surface area (MBET) / $\text{m}^2 \cdot \text{g}^{-1}$	749.4	955.6	1392.4	1694.2
Platinum content/%	4.9	8.1	12.3	14.1

The CV curves revealed a peak potential of 0.83 V for Pt/C. In addition, the peak of the experimental sample first decreased and then increased with the temperature, reaching the maximum 0.83 V of Pt-NC-900 (Fig. 5a). It is worth mentioning that although ICP showed that Pt-NC-1000 had the highest platinum content, its reduction peak lower than Pt-NC-900, the same conclusion was also proved in LSV (Fig. 5b), the half-wave potential of Pt-NC-900 was 0.84 V , even more than 20% Pt/C catalyst, while the half-wave potential of Pt-NC-1000 which was 0.80 V , this was mainly caused by the aggregation of Pt clusters and the reduction of active sites, which proves that Pt-NC-900 is the catalyst with the best catalytic activity. The rotating disk electrode is used to test at different speeds (Fig. 5c), and the data obtained is simulated by the K-L equation. The resultant curve was calculated and the electron transfer number n was 3.89, which proved that the reaction path was mainly along the four-electron transfer. Pt-NC-900 still showed a mass activity (0.207 A/mgPt) higher than 20% Pt/C (0.131 A/mgPt). Finally, its stability was investigated (Fig. 5d). After 5000 cycles, the half-wave of Pt-NC-900 The potential dropped by 70 mV .

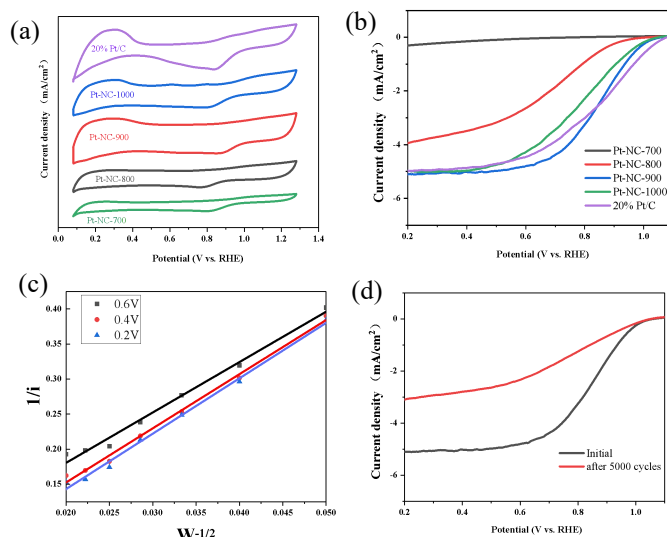


Fig. 5. (a) CV and (b) LSV curves of Pt/C, Pt-NC-700, Pt-NC-800, Pt-NC-900, Pt-NC-1000 in O_2 -saturated 0.1 M HClO_4 solution. (c) K-L plots of Pt-NC-900 recorded at different potential values. (d) Pt-NC-900 LSV comparison curve after 5000 cycles

4. CONCLUSION

In summary, we had successfully synthesized cubic ZIF-8 in the aqueous phase through the introduction of surfactants CTAB. The synthesis process achieved green synthesis without methanol. By controlling the heat treatment temperature and atmosphere strategy, we obtained large specific surface area and high pyridinic N content and high graphitization carbon support. The results showed that as the treatment temperature increases, the carrier's Pt-carrying capacity increased, but its activity did not increase further. The cubic ZIF-8 had the best ORR performance after heat treatment at 900 °C, which was attributed to a proper amount of defects and graphitization degree. Compared with commercial 20% Pt/C, it had less Pt usage, which improved Pt usage efficiency. This proved that CTAB water-phase synthesis ZIF-8 can be used as a carbon carrier with a lower Pt loading, thus reducing the cost of fuel cell catalysts and enhancing the possibility of fuel cell commercialization.

ACKNOWLEDGEMENT

The authors gratefully acknowledge the supports from the China Scholarship Council, Shanghai Automobile Industry Science and Technology Development FOUNDATION (1801).

REFERENCE

- [1] Guo D, Shibuya R, Akiba C, et al. Active sites of nitrogen-doped carbon materials for oxygen reduction reaction clarified using model catalysts[J]. *Science*, 2016, 351(6271): 361—365.
- [2] Wang X X, Hwang S, Pan Y T, et al. Ordered Pt₃Co Intermetallic Nanoparticles Derived from Metal-Organic Frameworks for Oxygen Reduction[J]. *Nano Lett*, 2018, 18(7): 4163—4171.
- [3] Zhang L, Zhang X F, Chen X L, et al. Facile solvothermal synthesis of Pt₇₁Co₂₉ lamellar nanoflowers as an efficient catalyst for oxygen reduction and methanol oxidation reactions[J]. *Journal of Colloid and Interface Science*, 2019, 536: 556—562.
- [4] Yang L, Zeng X, Wang W, et al. Recent Progress in MOF-Derived, Heteroatom-Doped Porous Carbons as Highly Efficient Electrocatalysts for Oxygen Reduction Reaction in Fuel Cells[J]. *Advanced Functional Materials*, 2018, 28(7).
- [5] Zhang L J, Su Z X, Jiang F L, et al. Highly graphitized nitrogen-doped porous carbon nanopolyhedra derived from ZIF-8 nanocrystals as efficient electrocatalysts for oxygen reduction reactions[J]. *Nanoscale*, 2014, 6(12): 6590—6602.
- [6] Jiang T, Luan W, Ren Y, et al. Synergistic heat treatment derived hollow-mesoporous-microporous Fe-N-C-SHT electrocatalyst for oxygen reduction reaction[J]. *Microporous and Mesoporous Materials*, 2020, 305: 110382.
- [7] Yang L, Xu G, Ban J, et al. Metal-organic framework-derived metal-free highly graphitized nitrogen-doped porous carbon with a hierarchical porous structure as an efficient and stable electrocatalyst for oxygen reduction reaction[J]. *J Colloid Interface Sci*, 2019, 535: 415-424.
- [8] Gu W L, Shang C S, Li J, et al. Nitrogen-Doped Porous Carbon Matrix Derived from Metal-Organic Framework-Supported Pt Nanoparticles with Enhanced Oxygen Reduction Activity[J]. *Chemelectrochem*, 2017, 4(11): 2814—2818.
- [9] Li Y, Wang F, Zhu H. Synthesis of H₂O₂ - CTAB dual-modified carbon black-supported Pt₃Ni to improve catalytic activity for ORR[J]. *Journal of Materials Science*, 2020, 55(25): 11241—11252.
- [10] Xue S, Yu Y, Wei S, et al. Nitrogen-doped porous carbon derived from ZIF-8 as a support of electrocatalyst for enhanced oxygen reduction reaction in acidic solution[J]. *Journal of the Taiwan Institute of Chemical Engineers*, 2018, 91: 539—547.